Crystal Structure of a Novel Red Copper Protein from *Nitrosomonas europaea*[†,‡]

Raquel L. Lieberman,[§] David M. Arciero,[||] Alan B. Hooper,[||] and Amy C. Rosenzweig*[,§]

Departments of Biochemistry, Molecular Biology, and Cell Biology and of Chemistry, Northwestern University, Evanston, Illinois 60208 and Department of Biochemistry, Molecular Biology, and Biophysics, University of Minnesota, St. Paul, Minneapolis 55108

Received February 6, 2001; Revised Manuscript Received March 14, 2001

ABSTRACT: Nitrosocyanin (NC) is a mononuclear red copper protein isolated from the ammonia oxidizing bacterium *Nitrosomonas europaea*. Although NC exhibits some sequence homology to classic blue copper proteins, its spectroscopic and electrochemical properties are drastically different. The 1.65 Å resolution crystal structure of oxidized NC reveals an unprecedented trimer of single domain cupredoxins. Each copper center is partially covered by an unusual extended β-hairpin structure from an adjacent monomer. The copper ion is coordinated by His 98, His 103, Cys 95, a single side chain oxygen of Glu 60, and a solvent molecule. In the 2.3 Å resolution structure of reduced NC, His 98 shifts away from the copper ion, and the solvent molecule is not observed. The arrangement of these ligands renders the coordination geometry of the NC red copper center distinct from that of blue copper centers. In particular, the red copper center has a higher coordination number and lacks the long Cu−S(Met) and short Cu−S(Cys) bond distances characteristic of blue copper. Moreover, the red copper center is square pyramidal whereas blue copper is typically distorted tetrahedral. Analysis of the NC structure provides insight into possible functions of this new type of biological copper center.

Blue copper proteins have intrigued bioinorganic chemists for the past 50 years. These small electron-transfer proteins contain a mononuclear blue, or type 1, copper center characterized by three unique features (*1*−*3*). First, the blue color results from an intense absorption band at ∼600 nm. Second, the copper center has a high redox potential as compared to aqueous inorganic copper complexes. Third, the electron paramagnetic resonance (EPR)[1] spectrum is unusual and differs significantly from that of inorganic Cu(II). The blue copper site is typically coordinated by a cysteine with a short Cu−S(Cys) bond and two histidines in a trigonal fashion. The 600 nm absorption band is attributed to S(Cys)-to-Cu(II) ligand-to-metal charge-transfer. In the prototypical blue copper protein plastocyanin, a methionine at a long distance completes the coordination, resulting in a distorted tetrahedral geometry (*4*). In other blue copper proteins, differences in the number of axial ligands afford trigonal bipyramidal (*5*) or trigonal planar (*6*, *7*) coordination. By contrast, mononuclear normal, or type 2, copper centers, found in superoxide dismutase (*8*) and in various enzymes with oxidase and oxygenase activities (*9*, *10*), are not deep blue in color and exhibit EPR spectral features and coordination geometry similar to inorganic square planar Cu(II) complexes (*11*).

Nitrosocyanin (NC) is a unique 112-residue mononuclear copper protein found in *Nitrosomonas europaea* (*12*), a chemoautotrophic bacterium that derives energy from the oxidation of ammonia to nitrite (*13*) and plays a key role in the nitrification branch of the global nitrogen cycle (*14*). NC exhibits some sequence homology to blue copper proteins such as plastocyanin and the electron transfer domain of nitrous oxide reductase (N_2OR), but its spectroscopic and electrochemical properties are drastically different (*12*, *15*). NC is brilliant red in color with an absorption band at 390 nm ($\epsilon = 4400\ M^{-1}\ cm^{-1}$). Its redox potential of +85 mV is well outside the range of +184 to +680 mV observed for blue copper (*3*). In addition, its EPR spectrum is more similar to that of normal copper (*16*). Because NC lacks all three properties traditionally associated with blue copper and its optical spectrum and sequence are not consistent with normal copper, its red copper site likely represents a new type of mononuclear copper center. To determine the molecular details of this novel red copper center and to gain insight into its biological function, we have determined the crystal structures of oxidized and reduced NC.

EXPERIMENTAL PROCEDURES

Crystallization and Data Collection. NC was purified from *N. europaea* as described elsewhere (*16*). The crystal used for a Cu multiwavelength anomalous dispersion (MAD) experiment was obtained by mixing 1 μL of purified NC at 30 mg/mL with an equal amount of precipitant solution containing 1.4 M trisodium citrate, 0.1 M Hepes pH 7.5, and 5% (v/v) Jeffamine M-600 at room temperature. Red crystals grew in sitting drops within 48 h to average

[†] This work was supported by funds from the David and Lucile Packard Foundation (A.C.R.), by NSF Grant DMB-9019687 (A.B.H.), and by DOE Grant DE-FG02-95ER20191 (A.B.H.). R.L.L. is supported in part by NIH training grant GM08382-10.

[‡] Refined coordinates have been deposited in the Protein Data Bank with accession codes 1IBY and 1IC0 for oxidized NC and 1IBZ for reduced NC.

* Address correspondence to this author. Telephone: (847) 467-5301. Fax: (847) 467-6489. E-mail: amyr@northwestern.edu.

[§] Northwestern University.

[||] University of Minnesota.

[1] Abbreviations: EPR, electron paramagnetic resonance; NC, nitrosocyanin; N_2OR, nitrous oxide reductase; MAD, multiwavelength anomalous dispersion; rms, root-mean-square; NiR, nitrite reductase; AO, ascorbate oxidase.

10.1021/bi0102611 CCC: $20.00 © 2001 American Chemical Society
Published on Web 04/17/2001

Table 1: Crystallographic Statistics

Data Collection and MAD Phasing

	NC-MAD					
	$\lambda 1$	$\lambda 2$	$\lambda 3$	$\lambda 4$	HIGHRES	REDUCED
wavelength (Å)[a]	1.41097	1.38035	1.37957	1.34954	0.989	0.946
resolution range (Å)	500−2.20	500−2.10	500−2.10	500−2.10	15.0−1.65	15.0−2.30
unique observations	41 463	46 668	47 691	48 519	58 664	23 593
total observations	570 947	653 668	654 294	654 370	361 955	128 504
completeness[b]	98.1 (99.6)	98.3 (99.7)	98.3 (99.7)	98.2 (99.7)	97.0 (95.2)	99.4 (99.3)
R_{sym}[c]	0.046 (0.180)	0.056 (0.253)	0.058 (0.256)	0.053 (0.226)	0.060 (0.343)	0.084 (0.325)
% > 3σ (I)	81.5 (53.4)	76.8 (42.9)	76.4 (42.9)	77.3 (45.1)	71.0 (20.5)	59.1 (21.4)
figure of merit[d]		0.79				

Refinement

	NC-MAD	HIGHRES	REDUCED
resolution (Å)	43.0−2.10	15.0−1.65	15.0−2.30
no. of protein atoms	5105	3452	3424
no. of copper ions	6	4	4
no. of water molecules	248	581	313
no. of hexanediol molecules	N/A	4	0
no. of reflections	87 277	58 042	22 318
R-factor[e]	0.216	0.186	0.180
R-free[f]	0.247	0.215	0.225
rms bond lengths	0.006	0.006	0.005
rms bond angles	1.4	1.6	1.4
average B-value (Å^2)	41.1	20.2	25.3

[a] All data sets were collected at the DND-CAT beamline at the Advanced Photon Source using a 2K × 2K Mar CCD detector. [b] Values in parentheses are for the highest resolution shell: λ_1, 2.28−2.2 Å; λ_2, λ_3, λ_4, 2.18−2.1 Å; HIGHRES, 1.71−1.65 Å; REDUCED, 2.38−2.3 Å. [c] $R_{sym} = \sum|I_{obs} - I_{avg}|/\sum I_{obs}$, where the summation is over all reflections. [d] Figure of merit was obtained from the program SOLVE for 20−3 Å resolution. [e] R-factor $= \sum|F_{obs}\text{-}F_{calc}|/\sum F_{obs}$. [f] Ten percent of the reflections were reserved for calculation of R-free for the NC-MAD structure and five percent for the HIGHRES and REDUCED structures.

dimensions of 0.3 × 0.3 × 0.5 mm (Figure 2a). The crystals belong to the space group $P2_12_12_1$ with unit cell dimensions $a = 90.9$ Å, $b = 92.7$ Å, and $c = 97.2$ Å. For data collection, an equal volume of cryosolvent containing 1.4 M trisodium citrate, 0.1 M Hepes pH 7.5, and 20% (w/v) sucrose was layered on top of a sitting drop containing mother liquor and a crystal. The crystal was then dragged vertically with a rayon loop from the mother liquor through the layer containing the cryosolvent and flash frozen in the nitrogen stream at −160 °C. This procedure was necessary because the NC crystals are not stable in cryosolvent for more than 20 s. The crystal used for high-resolution data collection was grown at room temperature by combining 1 μL of purified NC at 30 mg/mL with an equal amount of precipitant solution containing 1.4 M trisodium citrate, 0.1 M Hepes pH 7.5, and 3% (w/v) 1,6-hexanediol. Using this condition, large red crystals grew in sitting drops within 1−2 weeks. These crystals belong to the space group *R*32, with unit cell dimensions $a = b = 96.4$ Å and $c = 279.8$ Å. Crystals were mounted using the same cryosolvent and procedure as for the orthorhombic crystals and flash frozen in liquid nitrogen.

To obtain crystals of reduced NC, a 10 μL aliquot of 30 mg/mL NC was transferred to a Coy anaerobic chamber. Upon addition of 1 μL of a 30% (w/v) dithionite solution, the protein solution became colorless. Crystallization was carried out anaerobically using the same precipitant solution as for the oxidized *R*32 crystal form. The precipitant solution was degassed under vacuum for 1 h before transfer into the anaerobic box. Small colorless crystals that exhibited similar morphology to those obtained with oxidized protein appeared within three weeks. Like their oxidized counterparts, the reduced crystals belong to the space group *R*32, with unit cell dimensions of $a = b = 97.6$ Å and $c = 283.0$ Å. Crystals were prepared for data collection by transfer to 10 μL of a degassed solution containing 1.6 M trisodium citrate, 0.1 M Hepes pH 7.5, and 20% (w/v) sucrose in a 9-well glass plate. The drop containing the crystal and cryosolvent was then sealed and transferred out of the anaerobic box. The crystal was mounted on a rayon loop and flash cooled in liquid nitrogen within 20 s of removal from the chamber. All data were collected at −160 °C at the Dupont-Northwestern-Dow Collaborative Access Team (DND-CAT) beamline at the Advanced Photon Source using a 2K × 2K Mar CCD detector. The programs DENZO and SCALEPACK were used for data processing (*17*).

Structure Determination. Data for Cu MAD phasing were collected on an orthorhombic crystal (NC-MAD) at four wavelengths using the reverse beam technique (Table 1). The positions of the six copper ions were determined using the program SOLVE (*18*). An initial electron density map calculated to 3 Å resolution revealed continuous density corresponding to multiple β-strands and indicated that the six copper ions are arranged in two protein trimers (monomers labeled 1−6) in the asymmetric unit. The program O (*19*) was used to build models of the two trimers, and iterative cycles of simulated annealing and individual B-value refinement with CNS (*20*) followed by model rebuilding with O were performed using the free R-value to monitor the refinement progress (Table 1). The two protein trimers are related by a molecular 2-fold axis, and noncrystallographic symmetry restraints were imposed until the final cycle of refinement to 2.1 Å resolution. The final model consists of residues 2−111 for monomer 1, residues 2−112 for monomers 2, 3, 4, and 5, residues 3−112 for monomer 6, and 248 water molecules.

After completion of the 2.1 Å resolution structure, a 1.65 Å resolution data set was collected on a rhombohedral crystal (HIGHRES) (Table 1). Molecular replacement with the CCP4 program package (*21*) using the 2.1 Å resolution structure as a starting model located one trimer (monomers B, C, and D) in the asymmetric unit. A fourth monomer (labeled E) located near the crystallographic 3-fold axis was also evident in the resultant electron density map. Multiple cycles of refinement with CNS and model building with O yielded a final model consisting of residues 1−112 for each monomer, 581 water molecules, and 4 hexanediol molecules. The reduced NC structure (REDUCED) was refined using the refined HIGHRES oxidized structure without the copper ions as a starting model. The four copper ions were located as $\sim 15\sigma$ peaks in an $F_o - F_c$ difference electron density map. The final model includes residues 3−112 for monomers B, C, and D, residues 1−112 for monomer E, and 313 water molecules. Ramachandran plots generated with PROCHECK (*22*) show that the three models exhibit good geometry with all residues in the most favored and additionally allowed regions. Figures were generated with MOLSCRIPT (*23*), RASTER3D (*24*), and BOBSCRIPT (*25*).

RESULTS AND DISCUSSION

Overall Structure. Three NC monomers form a cylindrical trimer (Figure 1a,b), consistent with gel filtration data indicating that NC is oligomeric in solution (*16*). The NC-MAD (Table 1) asymmetric unit contains two protein trimers (monomers 1−6) whereas the HIGHRES asymmetric unit houses one trimer (monomers B, C, and D) plus a fourth monomer (monomer E) located near the crystallographic 3-fold axis. This monomer is part of a crystallographic trimer that is nearly identical to the noncrystallographic trimer. Each monomer comprises a flattened, eight-stranded β-barrel (β1, β3−β9) and an unusual β-hairpin structure (C-terminus of β1 and β2, residues 11−32) that extends from, but is not part of, the β-barrel structure (Figure 1a,c). There is one α-helical turn within the loop connecting β8 and β9. The hairpin is stabilized by side chain hydrogen bonding interactions on its solvent-exposed surface between Asp 12 and Arg 29 and between Asn 19 and Thr 24. On one end of the trimer, the three extended β-hairpins are arranged in a pinwheel structure. Each hairpin caps the copper site of an adjacent monomer, with the copper ion ∼16 Å from the top surface of the pinwheel (Figure 1a,b). A strong hydrogen bond between the side chains of Glu 21 on the hairpin and Ser 59 on the loop connecting strands β4 and β5 in an adjacent molecule stabilizes the hairpin conformation. The hairpin forms a hydrophobic cavity, ∼30 Å^2 in volume, lined by Ile 15, Leu 18, Val 20, Val 23, Val 25, and Ile 28 on the top surface, and Phe 31, Ile 102, and Ile 58 from the neighboring monomer on the bottom surface. In the HIGHRES structure, electron density modeled as a 1,6-hexanediol molecule from the crystallization solution is present in this pocket, ∼4.5 Å above the copper center (Figure 1d).

Besides the hydrogen bonding interaction between Glu 21 and Ser 59, there are several other intermonomer interactions involving residues located on the hairpin. The side chain of Thr 13 and the carbonyl oxygen of Ala 30 are linked to Asn 101, which is located on the α-helical turn of the adjacent molecule. In addition, the guanidinium group of Arg 29 interacts with the carbonyl oxygen atoms of Lys 26 and Asn 27 from an adjacent molecule. Other hydrogen bonding interactions between monomers include a salt bridge between Glu 36 and Lys 100, and interactions between the amide nitrogen of Thr 39 and the side chain oxygen of Thr 107. An ∼4 × 37 Å channel running parallel to the trimer axis is lined by alternating strata of hydrophobic and acidic residues from the three monomers. Starting at the opposite end of the trimer from the pinwheel structure, these residues include Val 111, Val 41, Thr 39, Thr 107, Glu 38, Leu 104, and Leu 34. The ring of three glutamic acid residues creates a region of negative charge in the middle of the channel.

The 10 independent crystallographic monomers from the two different crystal forms are very similar, with root-mean-square (rms) deviations for Cα atoms of 0.3−0.6 Å for all possible monomer−monomer superpositions. In all four monomers of the HIGHRES structure and in monomers 2, 3, 4, and 6 of the NC-MAD structure, the hairpin is bent ∼90° at Pro 16 and Asn 27. In monomers 1 and 5 of the NC-MAD structure, the hairpin is bent ∼120° and adopts a different conformation (Figure 1c) in which Glu 21 and Ser 59 from the adjacent molecule are not hydrogen bonded, but are ∼13 Å apart. The shifted position of monomer 1 is due to strong main chain hydrogen bonds between the two Asn 19 residues from monomers 1 and 4 and between Glu17 from monomer 1 and Glu 21 from monomer 4. Crystal packing interactions between monomer 5 and a symmetry related monomer 2 involving Glu 17, Asn 19, and Glu 21 account for the position of the hairpin in monomer 5. These changes in conformation suggest that part of the hairpin structure is flexible.

Structural Relatives. The β-barrel of the NC monomer exhibits a cupredoxin fold characteristic of single domain blue copper proteins involved in intermolecular electron transfer (*2*, *26*). A superposition of plastocyanin (*4*, *27*) and NC gives an rms difference of 2.0 Å for 78 Cα coordinates, and the two copper centers occupy similar positions within the overall fold. The copper ions in NC are less solvent accessible due to the hairpin structure, however. Other structurally related single domain cupredoxins include azurin (*5*), stellacyanin (*28*), and rusticyanin (*29*). The trimeric structure observed in NC is not conserved in any of these small cupredoxins, however. NC is thus the first oligomeric single domain cupredoxin.

NC also resembles the cupredoxin domains of numerous multicopper enzymes (*26*), including ascorbate oxidase (AO) (*30*), laccase (*6*), ceruloplasmin (*7*), nitrite reductase (NiR) (*31*), and N_2OR (*32*). All these enzymes except for N_2OR contain multiple cupredoxin domains derived from a single polypeptide chain. Superpositions of NC with the three cupredoxin domains of AO and laccase, the six cupredoxin domains of ceruloplasmin, the two cupredoxin domains of NiR, and the Cu_A domain of N_2OR give rms differences of ∼1.5 Å. In each enzyme, the blue copper site in one cupredoxin domain functions in intramolecular electron transfer to a catalytic copper center housed in a separate domain. The two copper centers are typically separated by ∼12 Å (*26*). Notably, each cupredoxin domain in ceruloplasmin contains an extended loop (35−40 residues) in the same position as the NC β-hairpin. These loop structures do not cover the blue copper centers in adjacent domains, however.

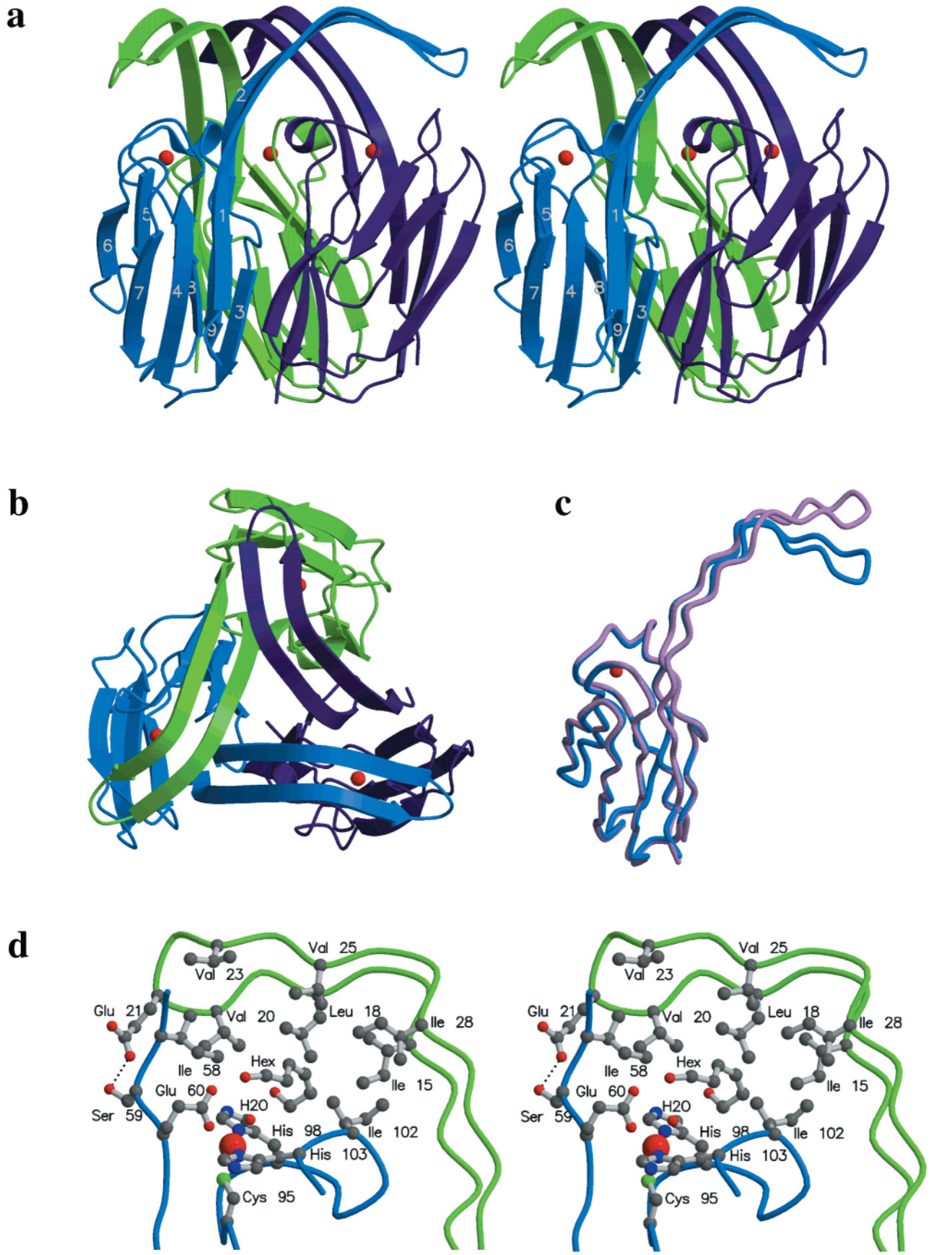

FIGURE 1: Structure of NC. (a) Stereoview of the NC trimer. The three monomers are shown in blue, green, and dark purple. Secondary structure elements are labeled on the blue monomer. (b) Viewed 90° from the orientation in panel a, looking down the molecular 3-fold axis. (c) Superposition of monomer B of the HIGHRES structure (blue) and monomer 5 of the NC-MAD structure (light purple). (d) Stereoview of the hydrophobic cavity above the copper center in the blue monomer formed by the β hairpin from the green monomer. The 1,6-hexanediol molecule is labeled Hex.

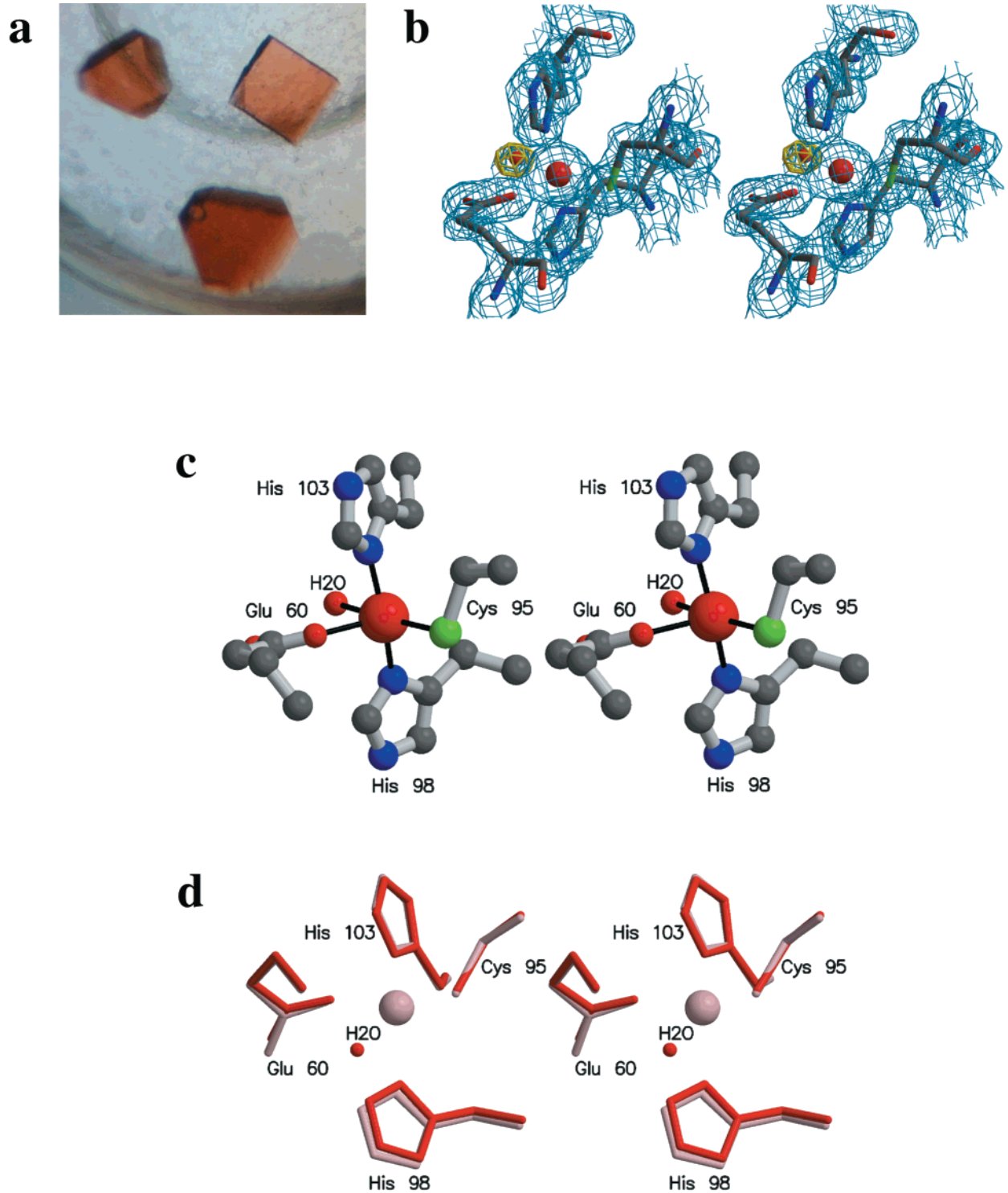

FIGURE 2: The NC red copper center. (a) Crystals of NC ($P2_12_12_1$ space group). (b) Stereoview of the final 1.65 Å resolution $2F_o - F_c$ electron density map (blue, contoured at 1.4σ) at the copper center. The copper ion is shown as a red sphere. The $F_o - F_c$ electron density map showing the coordinated water molecule is superimposed (yellow, contoured at 3.5σ). (c) Stereoview of the copper center. (d) Stereo superposition of the copper centers in oxidized (red) and reduced (pink) NC. The copper ion is only shown for reduced NC.

In addition to containing multiple domains, some multicopper enzymes are oligomeric, including AO and N_2OR (*32*), which are dimers, and NiR, which is a trimer (*33*). Unlike NC, the trimer interactions in NiR involve different domains. The N-terminal cupredoxin domain interacts with a C-terminal catalytic (also cupredoxin-like) domain from an adjacent monomer, and a catalytic type 2 copper site is located at the interface. NC lacks the corresponding additional domain and second copper site. NiR has an extended loop structure in the same position as the NC β-hairpin, but it is only 14 residues in length (*34*) as compared to 22 in NC. Whereas the NC β-hairpin is involved in trimer formation, the analogous loop in NiR interacts with the second domain in the same molecule and not with another monomer.

The Copper Center. Crystals of NC are red in color, indicating that the red copper center is intact (Figure 2a). Each monomer in the NC trimer houses one mononuclear

Table 2: Bond Distances and Angles in the NC Red Copper Center

	HIGHRES					REDUCED				
monomer	B	C	D	E	avg	B	C	D	E	avg
					Bond Lengths (Å)					
Cu-E60 Oϵ1	2.05	2.11	2.10	2.11	2.09	2.04	2.02	1.97	2.09	2.03
Cu−C95 Sγ	2.26	2.29	2.25	2.27	2.26	2.27	2.26	2.28	2.25	2.26
Cu−H98 Nδ	2.01	2.06	1.98	2.02	2.02	2.34	2.41	2.60	2.10	2.36
Cu−H103 Nδ	1.98	1.97	1.98	1.95	1.97	1.95	2.00	1.98	2.10	2.01
Cu−H_2O	2.06	2.42	2.38	2.15	2.25					
					Bond Angles (°)					
H98 Nδ−Cu−H103 Nδ	156	160	157	157	156	143	142	136	148	142
H98 Nδ−Cu-E60 Oϵ1	95	96	94	95	95	90	92	81	102	91
H98 Nδ−Cu−C95 Sγ	98	100	97	98	98	104	103	110	102	105
H103 Nδ−Cu−E60 Oϵ1	91	86	89	90	89	98	88	97	86	92
H103 Nδ−Cu−C95 Sγ	100	97	100	99	99	102	105	105	100	103
C95 Sγ−Cu−E60 Oϵ1	119	114	116	116	116	120	133	129	120	126
H_2O−Cu−H98 Nδ1	74	77	76	76	76					
H_2O−Cu−H103 Nδ1	84	82	86	83	84					
H_2O−Cu−C95 Sγ	162	165	161	167	164					
H_2O−Cu−E60 Oϵ1	78	80	83	76	79					

copper site, and each pair of copper ions is separated by ~23 Å. In the HIGHRES structure (Figure 2b,c), the copper ion is coordinated by the sulfur of Cys 95, the δ nitrogens of His 98 and His 103, a single carboxylate oxygen atom of Glu 60, and a solvent molecule. This solvent ligand was modeled as a water molecule, but could also be assigned as hydroxide. Cys 95, His 98, and His 103 are located on the loop between β8 and β9, and Glu 60 is located on the loop connecting β4 and β5. Of the ligands, His 98 is the most solvent exposed and is hydrogen bonded to a water molecule through its ϵ nitrogen. The other ligands are also stabilized by hydrogen bonding interactions. The Cys 98 side chain is hydrogen bonded to the amide nitrogens of Gly 61 and Leu 97. Similar interactions between the coordinated cysteine and amide nitrogens are observed in plastocyanin and other cupredoxins (*2*, *26*). The ϵ nitrogen of His 103 interacts with the side chain oxygen of Asn 35, and the uncoordinated oxygen of Glu 60 is hydrogen bonded to the side chain of Ser 56 and to the coordinated water molecule. In addition, the coordinated water molecule interacts directly with the 1,6-hexanediol molecule in each monomer.

The bond distances and angles for the four amino acid ligands agree well among the monomers in the asymmetric unit (Table 2). The coordination geometry is best described as square pyramidal with Glu 60 sitting at the pyramid apex and the pyramid base comprising the copper ion, Cys 95, His 98, and His 103 and the water molecule (Table 2, Figure 2c). The average His 98 Nδ−Cu−His 103 Nδ and H_2O−Cu−Cys 95 Sγ bond angles are 156° and 164°, respectively, and the other angles are close to 90° with the exception of the 116° Cys 95 Sγ−Cu−Glu 60 Oϵ1 angle. If the water molecule, which is less ordered than the other ligands (average B-value of 44 Å^2) and not observed in the NC-MAD and REDUCED structures, is excluded, the most idealized geometry is seesaw. In this geometry, the two histidines are axial. The equatorial ligands, Glu 60 and Cys 95, reside approximately perpendicular to the plane containing the two histidines and the copper ion and are nearly 120° apart.

Chemical reduction of NC leads to a loss of the red color, indicative of reduction to Cu(I). The structure of reduced NC (REDUCED, Table 1) is almost identical to that of the oxidized form with an rms deviation of 0.3 Å for 330 Cα coordinates in the trimer. The overall coordination geometries for the two copper centers are similar, although the solvent ligand is not observed in the reduced protein. The most noteworthy difference is the Cu−His 98 Nδ bond distance, which increases to an average value of 2.45 Å for monomers B, C, and D as compared to 2.02 Å in the oxidized structure (Table 2, Figure 2d). This difference in bond length is greater than experimental error. In these three monomers, the His 98 ring shifts by ~40°, lengthening the Cu−Nδ distance and further exposing the copper center to the hydrophobic cavity formed by the β-hairpin structure. This shift of His 98 is consistent with the preference of Cu(I) for a lower coordination number (*3*). Interestingly, a pH-dependent elongation of the analogous Cu−His Nδ bond in plastocyanin is observed upon reduction (*35*). Monomer E exhibits a Cu−His Nδ bond distance of 2.10 Å (Table 2), suggesting that it may be oxidized. One possibility is that the environment of His 98 in the crystallographic trimer is somehow different from that in the noncrystallographic trimer. His 98 occupies the same position and participates in the same hydrogen bonding interactions in both trimers, however. It is therefore unclear how monomer E could be oxidized selectively.

Red Copper Versus Blue Copper. Although NC structurally resembles blue copper proteins, the molecular details of red and blue copper centers are distinct. The two types of centers share three amino acid ligands, two histidines and one cysteine, but diverge in the remainder of their coordination spheres. Some blue copper centers are three-coordinate (*6*, *7*), but most have one or two additional weakly bound ligands. A common fourth ligand is a methionine with a Cu−S distance of 2.6−3.0 Å. One exception is stellacyanin, in which a glutamine at 2.2 Å replaces this axial methionine (*28*). In some azurins, a main chain carbonyl oxygen ~3.2 Å from the copper ion acts as a fifth donor (*3*). By contrast, the red copper center has four, rather than three, strong protein ligands, with a glutamic acid oxygen 2.09 Å from the copper ion. Furthermore, a coordinated water molecule with a Cu−O distances < 2.5 Å renders the oxidized red copper center five-coordinate (Table 2). Although His 98 and Cys 95 in NC are sequentially and structurally conserved between red and blue copper, His 103 in NC replaces the methionine in blue copper centers, and Glu 60 replaces the N-terminal histidine (Figure 3). A particularly striking

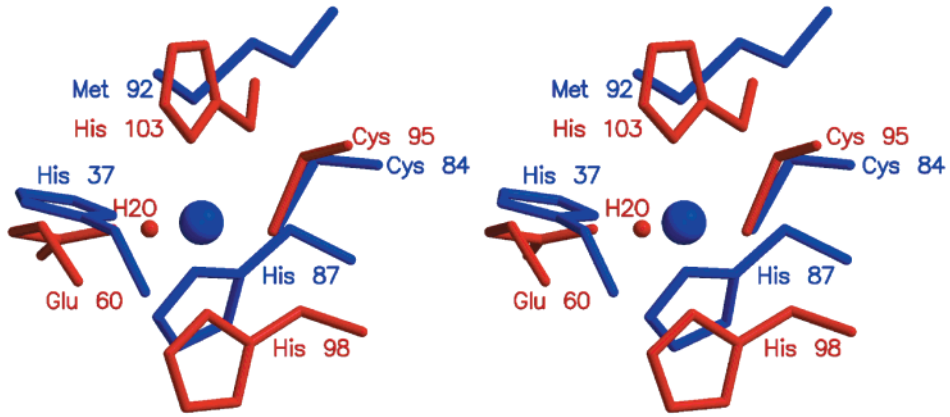

FIGURE 3: Stereo comparison of red copper and blue copper. The plastocyanin blue copper center (blue, PDB accession code 1PLC) is superimposed on the NC red copper center (red) such that the two copper ions occupy the same position. The copper ion is only shown for plastocyanin.

difference between red and blue copper is the Cu−S(Cys) bond distance. In blue copper, with the exception of some azurins (*2*, *3*) and the subfamily of basic blue proteins (*36*, *37*), the Cu−S(Cys) distance is short, ~2.1 Å (*4*), and is responsible for the blue color (*1*). The 2.26 Å distance observed in NC is similar to that observed in five-coordinate inorganic copper compounds (*38*).

The differences in ligand identity and bond lengths between red and blue copper result in distinct coordination geometries. Classic blue copper centers are distorted tetrahedral or trigonal pyramidal, with a methionine sulfur capping the pyramid (*4*). Blue copper sites that lack any additional weak ligands are trigonal planar (*6*, *7*), and those that have two distant donors, the methionine sulfur and a carbonyl oxygen, are trigonal bipyramidal (*5*). By contrast, the NC red copper center is square pyramidal. This tetragonal distortion arises from a significant displacement of NC His 98 relative to its blue copper counterpart. A superposition of NC and plastocyanin shows that His 98 and the corresponding histidine in plastocyanin, His 87, occupy different positions. His 98 is almost collinear with His 103, resulting in the square plane formed by His 98, His 103, Cys 95, and the water molecule as compared to the trigonal plane formed by His 87, His 37, and Cys 84 in plastocyanin (Figure 3). The tetragonal geometry is consistent with the NC EPR spectrum, which exhibits hyperfine splitting more characteristic of normal, tetragonal copper (*16*). The NC ligand set and geometry probably also explain the intense absorption band at 390 nm, but detailed spectroscopic analysis is required to define the electronic structure of the red copper site.

The spectroscopic properties of NC are reminiscent of azurin (*39*, *40*) and rusticyanin (*41*) mutants in which the methionine residue has been replaced with glutamic acid. In these mutants, a 570-nm absorption band corresponding to a blue color dominates at low pH, and a 413-nm band corresponding to a brown color dominates at high pH. The increase in intensity at 413 nm is accompanied by the appearance of an EPR signal characteristic of normal, tetragonal copper. Although the NC red copper center is spectroscopically similar to the high pH forms of these mutants, the coordination environment is still markedly different. Instead of simply substituting glutamic acid for methionine, engineering of a red copper center would require two changes, replacement of the methionine with histidine and replacement of the N-terminal histidine with glutamic acid (Figure 3). In addition, the Cu−S(Cys) bond distance for the azurin mutant (*39*) is shorter than that in red copper, and the coordination geometry is very similar to that of wild-type azurin (*40*). Furthermore, the mutant redox potentials (*40*, *41*), although decreased, still fall at the lower limits of the range expected for blue copper (*3*).

Functional Implications. Since NC is present at a concentration comparable to that of essential metabolic enzymes in *Nitrosomonas europaea* (*12*), it probably has an important biological function. The structural similarity to cupredoxin domains suggests that NC might function in electron transfer. Because NC comprises single cupredoxin domains, intermolecular rather than intramolecular electron transfer is most likely. Intermolecular electron transfer would require docking sites for donor and acceptor proteins. In plastocyanin, two surface patches are proposed to interact with physiological reaction partners, a hydrophobic patch near copper ligand His 87 and an acidic patch comprising six negatively charged residues (*42*). A hydrophobic patch is also present in the NC trimer near His 98. This region includes residues Val 10, Phe 31, Val 33, Pro 57, Ile 58, Leu 97, Pro 99, and Ile 102. Interactions between some of these residues and hydrophobic residues from the β-hairpin of an adjacent monomer generate a hydrophobic cavity (Figure 1d). A conformational change in the hairpin, which is apparently flexible (Figure 1c), would expose the hydrophobic patch and facilitate docking with another protein, perhaps also a trimer. A second potential docking site is a surface groove formed at the monomer−monomer interfaces. There are three such grooves in the NC trimer. In these grooves, Tyr 11 and Glu 36 from one molecule interact with Lys 100 from an adjacent molecule. Located ~12 Å from both the copper center in the same monomer and that in the adjacent monomer, Tyr 11 is well positioned for electron transfer to either copper center. Another potentially important residue in this groove region is Trp 94, which is located ~4 Å from the Tyr 11−Glu 36−Lys 100 trio and 9 Å from the copper center in the same monomer.

Although the overall structure of NC is potentially consistent with a role in electron transfer, some properties of the copper center are less compatible with such a function. The trigonal coordination geometry of the blue copper center

destabilizes Cu(II) relative to Cu(I), increasing the redox potential and lowering the reorganization energy for electron transfer (*3*). In addition, exclusion of water from blue copper centers is proposed to contribute to the low reorganization energy (*3*). By contrast, the higher coordination number and tetragonal geometry of the red copper center favor Cu(II) and explain the low redox potential of NC. Furthermore, the red copper site contains a coordinated water molecule.

Since tetragonal copper centers are typically associated with catalysis (*9*, *10*), NC could also be an enzyme. The coordinated water molecule delineates an open coordination site for substrate binding, and the hydrophobic cavity formed by the β-hairpin structure is suggestive of an active site. In the oxidized structure, a 1,6-hexanediol molecule is trapped in this cavity <5 Å from the copper ion, indicating that a substrate could be accommodated near the copper center. In this scenario, the hydrophobic patch is not a docking site, but the surface groove could still represent a docking site for a partner protein. Determination of the function of the NC red copper center requires further biochemical characterization and may benefit from completion of the *Nitrosomonas europaea* genome.

ACKNOWLEDGMENT

We thank A. Chander for assistance with crystallization and A. Lamb for helpful discussions. The DND-CAT Synchrotron Research Center at the Advanced Photon Source is supported by the E.I. DuPont de Nemours & Co., The Dow Chemical Company, the NSF, and the State of Illinois.

REFERENCES

1. Solomon, E. I., Baldwin, M. J., and Lowery, M. D. (1992) *Chem. Rev. 92*, 521−542.
2. Messerschmidt, A. (1998) *Struct. Bonding 90*, 37−68.
3. Gray, H. B., Malmström, B. G., and Williams, R. J. P. (2000) *J. Biol. Inorg. Chem. 5*, 551−559.
4. Guss, J. M., Bartunik, H. D., and Freeman, H. C. (1992) *Acta Crystallogr. B48*, 790−811.
5. Dodd, F. E., Abraham, Z. H. L., Eady, R. R., and Hasnain, S. S. (2000) *Acta Crystallogr. D56*, 690−696.
6. Ducros, V., Brzozowski, A. M., Wilson, K. S., Brown, S. H., Østergaard, P., Schneider, P., Yaver, D. S., Pederson, A. H., and Davies, G. J. (1998) *Nat. Struct. Biol. 5*, 310−316.
7. Zaitseva, I., Zaitsev, V., Card, G., Moshkov, K., Bax, B., Ralph, A., and Lindley, P. (1996) *J. Biol. Inorg. Chem. 1*, 15−23.
8. Bertini, I., Mangani, S., and Viezzoli, M. S. (1997) *Adv. Inorg. Chem. 45*, 127−250.
9. Klinman, J. P. (1996) *Chem. Rev. 96*, 2541−2562.
10. Solomon, E. I., Sundaram, U. M., and Machonkin, T. E. (1996) *Chem. Rev. 96*, 2563−2605.
11. Solomon, E. I., Lowery, M. D., LaCroix, L. B., and Root, D. E. (1993) *Methods Enzymol. 226*, 1−33.
12. Whittaker, M., Bergmann, D., Arciero, D., and Hooper, A. B. (2000) *Biochim. Biophys. Acta 1459*, 346−355.
13. Hooper, A. B., Vannelli, T., Bergmann, D. J., and Arciero, D. M. (1997) *Antonie van Leeuwenhoek 71*, 59−67.
14. Richardson, D. J., and Watmough, N. J. (1999) *Curr. Op. Chem. Biol. 3*, 207−219.
15. Hooper, A. B., and Arciero, D. M. (1999) *J. Inorg. Biochem. 74*, 166.
16. Arciero, D. M., and Hooper, A. B., manuscript in preparation.
17. Otwinowski, Z., and Minor, W. (1997) *Methods Enzymol. 276*, 307−326.
18. Terwilliger, T. C., and Berendzen, J. (1999) *Acta Crystallogr. D55*, 849−861.
19. Jones, T. A., Zou, J.-Y., Cowan, S. W., and Kjeldgaard, M. (1991) *Acta Crystallogr. A47*, 110−119.
20. Brünger, A. T., Adams, P. D., Clore, G. M., DeLano, W. L., Gros, P., Grosse-Kunstleve, R. W., Jiang, J.-S., Kuszewski, J., Nilges, M., Pannu, N. S., Read, R. J., Rice, L. M., Simonson, T., and Warren, G. L. (1998) *Acta Crystallogr. D54*, 905−921.
21. Collaborative Computational Project, Number 4 (1994) *Acta Crystallogr. D50*, 760−763.
22. Laskowski, R. A. (1993) *J. Appl. Crystallogr. 26*, 283−291.
23. Kraulis, P. J. (1991) *J. Appl. Crystallogr. 24*, 946−950.
24. Merritt, E. A., and Bacon, D. J. (1997) *Methods Enzymol. 277*, 505−524.
25. Esnouf, R. M. (1997) *J. Mol. Graph. Model. 15*, 132−134.
26. Adman, E. T. (1991) *Adv. Protein Chem. 42*, 145−197.
27. Colman, H. C., Freeman, H. C., Guss, J. M., Murata, M., Norris, V. A., Ramshaw, J. A. M., and Venkatappa, M. P. (1978) *Nature 272*, 319−324.
28. Hart, P. J., Nersissian, A. M., Herrmann, R. B., Nalbandyan, R. M., Valentine, J. S., and Eisenberg, D. (1996) *Protein Sci. 5*, 2175−2183.
29. Walter, R. L., Ealick, S. E., Friedman, A. M., Blake, R. C., II, Proctor, P., and Shoham, M. (1996) *J. Mol. Biol. 263*, 730−751.
30. Messerschmidt, A., Ladenstein, R., Huber, R., Bolognesi, M., Avigliano, L., Petruzzelli, R., Rossi, A., and Finazzi-Agro, A. (1992) *J. Mol. Biol. 224*, 179−205.
31. Godden, J. W., Turley, S., Teller, D. C., Adman, E. T., Liu, M. Y., Payne, W. J., and LeGall, J. (1991) *Science 253*, 438−442.
32. Brown, K., Tegoni, M., Prudêncio, M., Pereira, A. S., Besson, S., Moura, J. J., Moura, I., and Cambilleau, C. (2000) *Nat. Struct. Biol. 7*, 191−195.
33. Suzuki, S., Kataoka, K., and Yamaguchi, K. (2000) *Acc. Chem. Res. 33*, 728−735.
34. Murphy, M. E., Turley, S., and Adman, E. T. (1997) *J. Biol. Chem. 272*, 28455−28460.
35. Guss, J. M., Harrowell, P. R., Murata, M., Norris, V. A., and Freeman, H. C. (1986) *J. Mol. Biol. 192*, 361−387.
36. LaCroix, L. B., Randall, D. W., Nersissian, A. M., Hoitink, C. W. G., Canters, G. W., Valentine, J. S., and Solomon, E. I. (1998) *J. Am. Chem. Soc. 120*, 9621−9631.
37. Einsle, O., Mehrabian, Z., Nalbandyan, R., and Messerschmidt, A. (2000) *J. Biol. Inorg. Chem. 5*, 666−672.
38. Holmes, R. R. (1984) *Prog. Inorg. Chem. 32*, 119−236.
39. Strange, R. W., Murphy, L. M., Karlsson, B. G., Reinhammar, B., and Hasnain, S. S. (1996) *Biochemistry 35*, 16391−16398.
40. Karlsson, B. G., Tsai, L.-C., Nar, H., Sanders-Loehr, J., Bonander, N., Langer, V., and Sjölin, L. (1997) *Biochemistry 36*, 4089−4095.
41. Hall, J. F., Kanbi, L. D., Strange, R. W., and Hasnain, S. S. (1999) *Biochemistry 38*, 12675−12680.
42. Redinbo, M. R., Yeates, T. O., and Merchant, S. (1994) *J. Bioenerg. Biomembr. 26*, 49−66.

BI0102611